

## Supporting Information

### **In-situ construction of ZnIn<sub>2</sub>S<sub>4</sub>/CdIn<sub>2</sub>S<sub>4</sub> 2D/3D nano hetero-structure for enhanced visible-light-driven hydrogen production**

Xinyu Dang<sup>a</sup>, Mingsen Xie<sup>a</sup>, Fangfang Dai<sup>a</sup>, Jinna Guo<sup>a</sup>, Jia Liu<sup>\*a,c</sup>, Xiaoquan Lu<sup>\*b</sup>

<sup>a</sup> *Tianjin Key Laboratory of Molecular Optoelectronic, Department of Chemistry, school of science, Tianjin University, Tianjin, 300072, P. R. China.*

<sup>b</sup> *Key Laboratory of Bioelectrochemistry & Environmental Analysis of Gansu Province, College of Chemistry & Chemical Engineering, Northwest Normal University, Lanzhou 730070, P. R. China.*

<sup>c</sup> *Key Laboratory of Advanced Energy Materials Chemistry (Ministry of Education), College of Chemistry, Nankai University, Tianjin 300071, China*

\* E-mail: liujia@tju.edu.cn, luxq@nwnu.edu.cn.

## **Experimental section**

### **Chemicals**

Zinc chloride ( $\text{ZnCl}_2$ ,  $\geq 99.95\%$ ), thioacetamide (TAA,  $\geq 99.00\%$ ), cadmium chloride hemi(pentahydrate) ( $\text{CdCl}_2 \cdot 2.5\text{H}_2\text{O}$ ,  $\geq 99.95\%$ ), absolute ethanol ( $\text{C}_2\text{H}_5\text{OH}$ , 99.80%), anhydrous sodium sulfite ( $\text{Na}_2\text{SO}_3$ ,  $\geq 98.00\%$ ), anhydrous sodium sulfate ( $\text{Na}_2\text{SO}_4$ , 99.99%) and sodium sulfide nine hydrate ( $\text{Na}_2\text{S} \cdot 9\text{H}_2\text{O}$ , 99.99%) were all purchased from Shanghai Aladdin Biochemical Technology Co., Ltd. Indium nitrate hexahydrate ( $\text{In}(\text{NO}_3)_3 \cdot 6\text{H}_2\text{O}$ , 99.99%) was purchased from Ailan (Shanghai) Chemical Technology Co., Ltd. The fluorine-doped tin oxide (FTO) glasses were purchased from Zhuhai Kaivo Optoelectronic Technology Co., Ltd. All reagents were used without further purification. The deionized (DI) water with a resistivity of  $18.2 \text{ M}\Omega \cdot \text{cm}$  was obtained from the Millipore Milli-Q water purification system.

### **Fabrication of $\text{ZnIn}_2\text{S}_4$ nanosheets**

In a typical experiment,  $\text{ZnIn}_2\text{S}_4$  nanosheets were synthesized by a solvothermal method. 0.0545 g  $\text{ZnCl}_2$  (0.4 mmol), 0.3271 g  $\text{In}(\text{NO}_3)_3 \cdot 6\text{H}_2\text{O}$  (0.8 mmol) and 0.2402 g TAA (1.6 mmol) were dissolved in 15 mL water and 15 mL ethanol under continuous stirring for 1 h. Then, the mixture was transferred to a 50 mL Teflon-lined autoclave and kept at  $180^\circ\text{C}$  for 24 h. After natural cooling to room temperature, the precipitate was collected by centrifugation and washed with deionized water and ethanol for several times, respectively. Finally, the obtained products were dried at room temperature in a vacuum oven for 12 h.

### **Fabrication of $\text{CdIn}_2\text{S}_4$ Nanocrystals**

0.0913 g  $\text{CdCl}_2 \cdot 2.5\text{H}_2\text{O}$  (0.4 mmol), 0.3271 g  $\text{In}(\text{NO}_3)_3 \cdot 6\text{H}_2\text{O}$  (0.8 mmol) and 0.2402 g TAA (1.6 mmol) were dissolved in 15 mL water and 15 mL ethanol under continuous stirring for 1 h. Subsequently, the mixture was transferred to a 50 mL Teflon-lined autoclave and kept at  $180^\circ\text{C}$  for 24 h. After naturally cooling down to room temperature, the product was washed with water and ethanol for several times followed by centrifugation and finally collected after drying at room temperature for 12 h in a vacuum oven.

### **Fabrication of $\text{ZnIn}_2\text{S}_4/\text{CdIn}_2\text{S}_4$ (ZCIS) nanocomposites**

$\text{ZnIn}_2\text{S}_4/\text{CdIn}_2\text{S}_4$  nano-composites were fabricated via a hydro-thermal process. In a typical procedure, 0.3271 g  $\text{In}(\text{NO}_3)_3 \cdot 6\text{H}_2\text{O}$  (0.8 mmol), 0.2402 g TAA (1.6 mmol), calculated amounts of  $\text{CdCl}_2 \cdot 2.5\text{H}_2\text{O}$  and  $\text{ZnCl}_2$  (sum of mole number equals to 0.4 mmol) were dissolved in 15 mL water and 15 mL ethanol. After being stirred for 1 h, the solution was transferred to a 50 mL

Teflon-lined stainless-steel autoclave and maintained at 180 °C for 24 h. After naturally cooling down to room temperature, the suspension was collected by centrifugation, washed with deionized water and ethanol for several times, respectively. Finally, the obtained products were dried at room temperature in a vacuum oven for 12 h. In the experiment, ZnIn<sub>2</sub>S<sub>4</sub>/CdIn<sub>2</sub>S<sub>4</sub> nanocomposites with different molar ratio of Cd/Zn in the reaction precursor were synthesized and labeled as ZCIS-10, ZCIS-30, ZCIS-50 and ZCIS-70 .

### **Characterization methods**

The Brunauer-Emmett-Teller (BET) specific surface area and pore size distribution of photocatalyst were obtained by using two-station automatic specific surface area and pore size analyzer (Autosorb-iQ2-MP, Quantachrome). Before measuring N<sub>2</sub> adsorption, the samples were degassed at 150 ° C for 8 h. Powder X-ray diffractometer (Smart Lab 9kW, Rigaku) was used to characterize the crystal structure of the product. The Cu K $\alpha$  was used as the target source ( $\lambda = 1.5406 \text{ \AA}$ ), the scanning speed was 6° min<sup>-1</sup> and the scanning range was 10-80°. The UV-visible diffuse reflectance spectrum (UV-vis DRS) of the sample was recorded by UV-3600 Plus UV-VIS-NIR spectrophotometer (Shimadzu), and BaSO<sub>4</sub> was used as reference. The detailed microstructure and morphology of the photocatalyst were characterized by a Talos F200X high resolution field emission transmission electron microscope (FEI), along with energy dispersive X-ray spectroscopy (EDX) element mapping data. SEM imaging was performed on a Verios 460L ultra-high resolution field emission scanning electron microscope (FEI). The Zeta potential of the sample was measured on a nano-particle size and Zeta potential analyzer (Zetasizer nano ZS90, Malvern Panalytical). The electron spin resonance (ESR) spectrum of the sample was obtained by JES-FA200 electron spin paramagnetic resonance spectroscopy. Thermo Fisher Scientific ESCALAB 250Xi+ X-ray photoelectron spectroscopy was used to analyze the binding energy of Zn, Cd, In, S elements and valence band (VB). All binding energies were calibrated to the C1s peak of amorphous surface carbon at 284.8 eV. The atomic ratios of Zn, Cd, In and S in the samples were measured by inductively coupled plasma mass spectrometry on an Agilent 7700x ICP-MS spectrometer. Photoluminescence (PL) spectra of the samples were obtained by an Edinburgh integrated steady-state transient fluorescence spectrometer (FS5, Edinburgh Instruments) at an excitation wavelength of 450 nm. The time-resolved photoluminescence (TRPL) decay curves were obtained by an FLS920 fluorescence lifetime spectrophotometer

(Edinburgh instruments, UK) under the excitation of hydrogen flash lamp with a wavelength 405 nm.

### **Evaluation of Photocatalytic hydrogen evolution**

A 300 W Xe lamp with a 420 nm cut-off filter was used as the visible light source. The photocatalytic H<sub>2</sub> evolution reactions were carried out in a Pyrex photo-reactor, which was connected to a closed gas circulation and evacuation system at ambient temperature. In a typical photocatalytic experiment, 4 mg of the obtained various photocatalyst powder was dispersed in 40 mL of an aqueous solution containing 0.25 M Na<sub>2</sub>SO<sub>3</sub> and 0.35 M Na<sub>2</sub>S as the sacrificial electron donor. Then the mixture was sonicated for 1 h at room temperature to get a homogeneous suspension. Prior to light irradiation, the reaction system was degassed by bubbling with high-purity nitrogen for 30 min to thoroughly remove air. During the photocatalytic reaction, the reactor was kept under constant agitation. The amount of hydrogen produced was analyzed by an online gas chromatograph (SP-2100A, TCD detector, argon as carrier gas, 5Å molecular sieve column). In order to evaluate the stability and reusability of photocatalytic hydrogen production, cyclic experiments were carried out under the same conditions. The apparent quantum yield (AQE) of ZCIS-50 sample was measured under the same reaction conditions except that using various band-pass filters of 420 nm, 450 nm, 475 nm, 500 nm, 550 nm and 600 nm to obtain monochromatic light. The AQE can be calculated according to the following equation:

$$AQE(\%) = \frac{2 \times \text{number of evolved hydrogen molecules}}{\text{number of incident photos}}$$

### **Photoelectrochemical measurements**

The electrochemical impedance (EIS) test was carried out on the Autolab electrochemical workstation (Metrohm, Switzerland) at an open circuit potential in the range from 10<sup>-2</sup> Hz to 10<sup>6</sup> Hz, with an amplitude of 5 mV. The photocatalyst was subjected to linear scanning voltammetry (LSV) and photocurrent response on the CHI660E electrochemical workstation (Chenhua, China). A 300 W Xe lamp equipped with a 420 nm cut off filter was used as the exciting light source for photocurrent measurement. All the measurements were performed in Na<sub>2</sub>SO<sub>4</sub> solution (0.2 M, PH = 6.8), and Ag/AgCl (saturated KCl) electrode was used as the reference electrode, graphite sheet was used as the counter electrode and the photocatalyst coated on fluoride tin oxide (FTO) was used as the working electrode in the conventional three-electrode cell. Linear scanning voltammetry (LSV) was carried out at a scan rate of 5

mV/s under visible light irradiation. FTO glasses were washed by sonicating sequentially in ultrapure water, ethanol and acetone for 30 minutes, and then dried with nitrogen. The working electrode was prepared as follows: 4 mg of the photocatalyst was dispersed in 2 mL of ultrapure water and sonicated for 1 h to form a uniform suspension. 100  $\mu$ L of the suspension was dropped onto a clean tin fluoride doped (FTO) glass substrate having an active area of  $1.0 \times 1.0 \text{ cm}^2$ , and then dried in air at  $100 \text{ }^\circ\text{C}$  for 12 h to obtain the working electrode.

### **Calculate Section**

When carried out DFT calculation, Perdew-Burke-Ernzerhof (PBE) exchange-correlation functional was used with a plane wave pseudopotential implementation. The kinetic energy cutoff was set to 380 eV. The (001) facet of  $\text{CdIn}_2\text{S}_4$  and  $\text{ZnIn}_2\text{S}_4$  was selected to construct heterojunction as model. The model was a periodic unit cell ( $1 \times 1 \times 1$ ). k-point of ( $3 \times 3 \times 1$ ) was adopted. All atoms were completely relaxed to obtain accurate structure. When calculated free energy for each transition state as  $\Delta G = \Delta E_0 - \Delta \text{ZPE} + \int \Delta C_p dT - T \Delta S$ , where  $\Delta G$  is the free energy change,  $\Delta E_0$  is the energy change of each state calculated at 0 K.  $\Delta \text{ZPE}$  is the variation in zero point energies (ZPE).  $C_p$  is heat capacity of each component.  $\Delta S$  is the entropy change of the reaction. Entropy and  $C_p$  value of each state was obtained by vibration analysis.

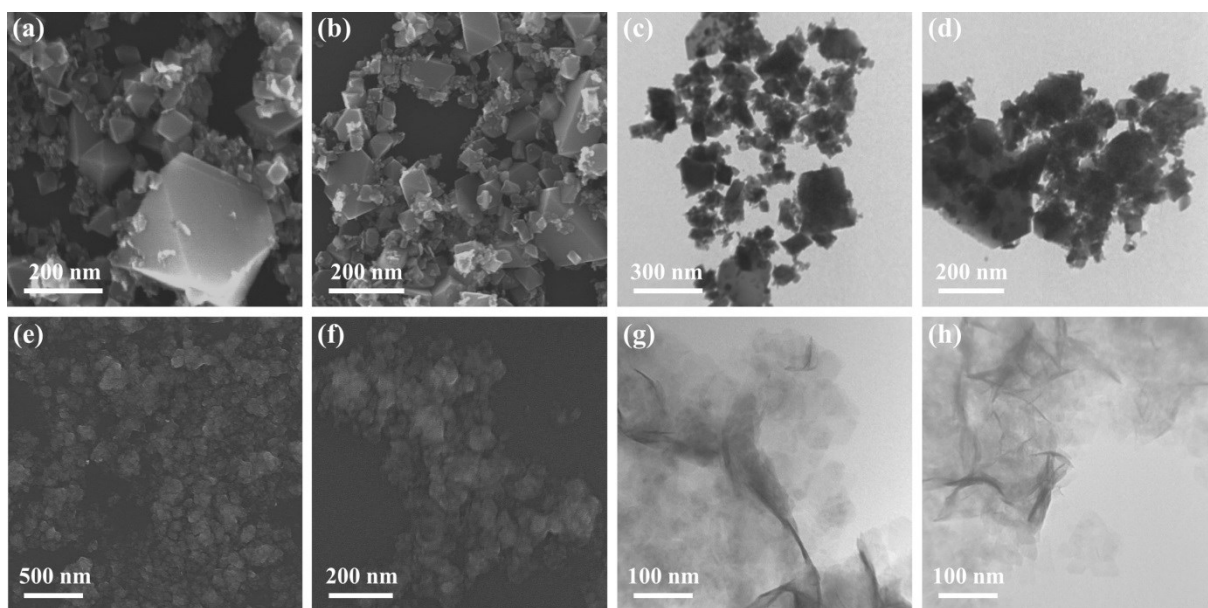


**Figure S1.** SEM images of (a, b)  $\text{CdIn}_2\text{S}_4$  and (e, f)  $\text{ZnIn}_2\text{S}_4$ . TEM images of (c, d)  $\text{CdIn}_2\text{S}_4$  and (g, h)  $\text{ZnIn}_2\text{S}_4$ .

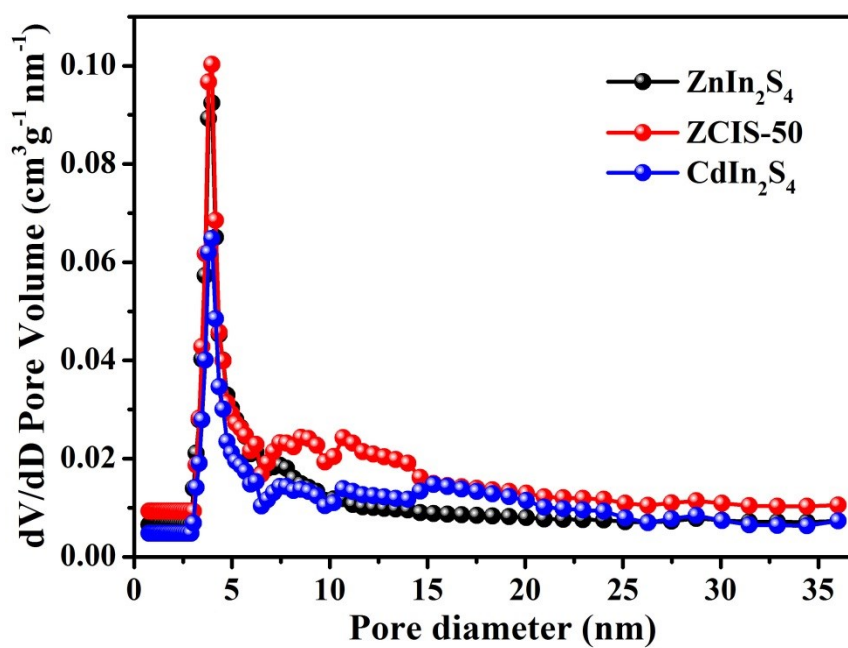


**Figure S2.** Pore size distribution curves of pure  $\text{ZnIn}_2\text{S}_4$ ,  $\text{CdIn}_2\text{S}_4$ , and ZCIS-50.

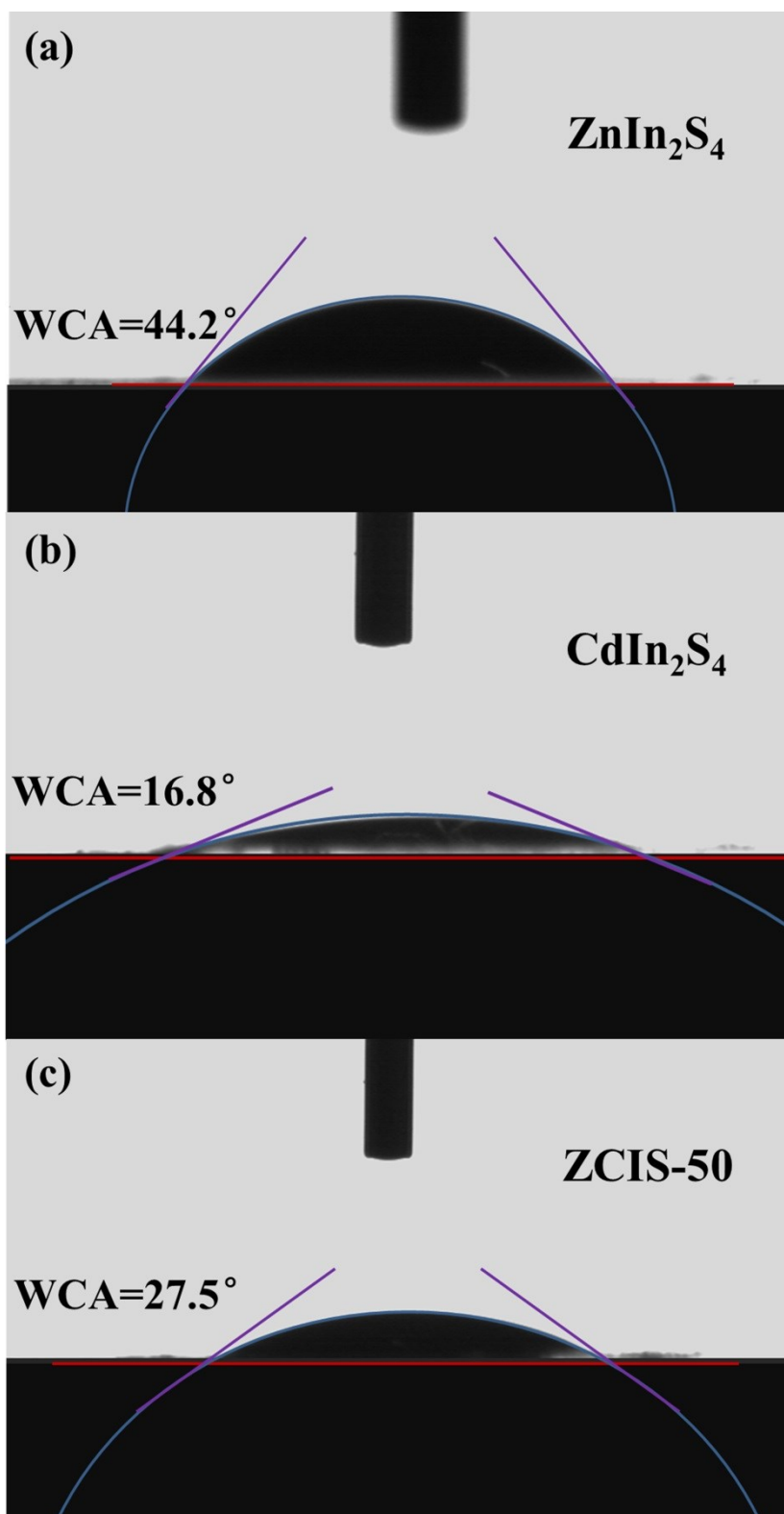


**Figure S3.** Static water contact-angle measurement of (a)  $\text{ZnIn}_2\text{S}_4$ , (b)  $\text{CdIn}_2\text{S}_4$ , and (c) ZCIS-50.

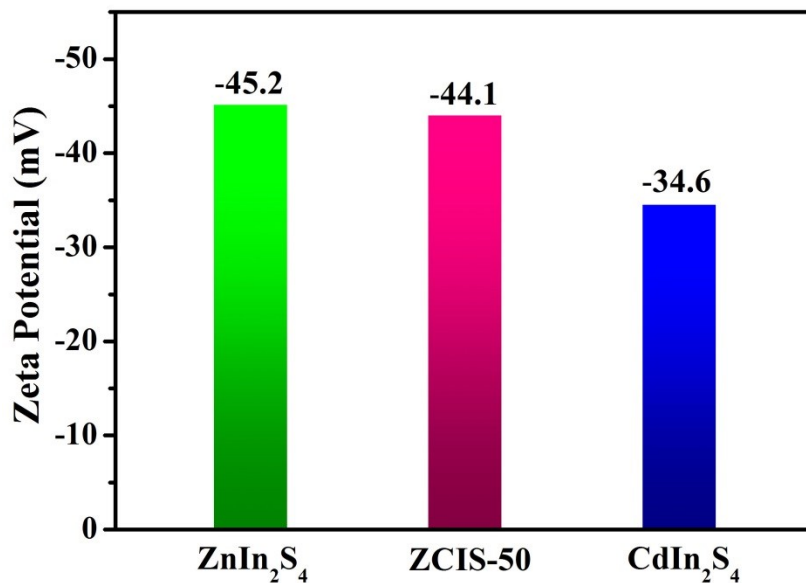


**Figure S4.** Zeta potentials of pure ZnIn<sub>2</sub>S<sub>4</sub>, CdIn<sub>2</sub>S<sub>4</sub>, and ZCIS-50 in water.

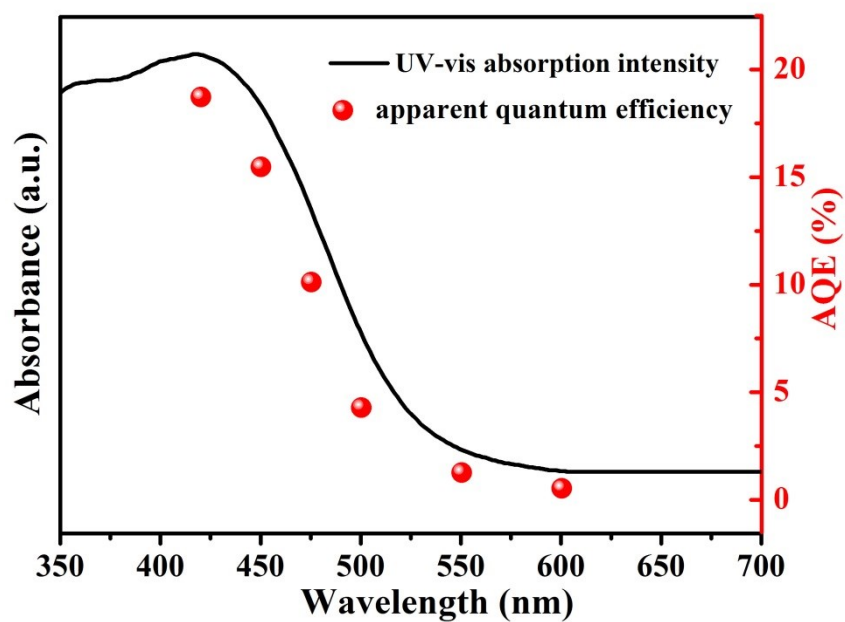


**Figure S5.** Wavelength dependence of apparent quantum efficiency (AQE) plot of ZCIS-50 for the photocatalytic H<sub>2</sub> evolution (right axis) and UV-vis absorption spectrum of ZCIS-50 (left axis).

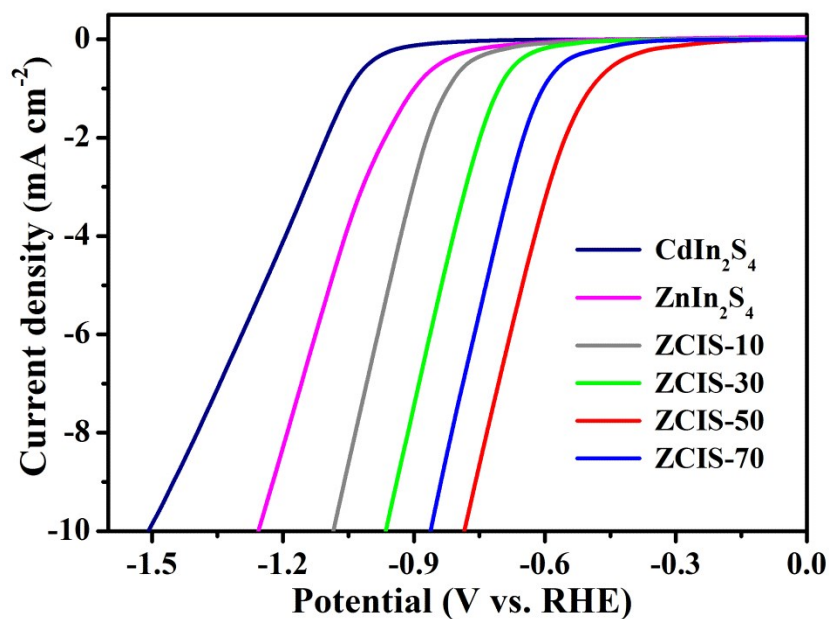


**Figure S6.** Polarization curves of ZnIn<sub>2</sub>S<sub>4</sub>, ZCIS-10, ZCIS-30, ZCIS-50, ZCIS-70, and CdIn<sub>2</sub>S<sub>4</sub> samples coated on FTO in 0.2 M Na<sub>2</sub>SO<sub>4</sub> aqueous solution under visible light irradiation.

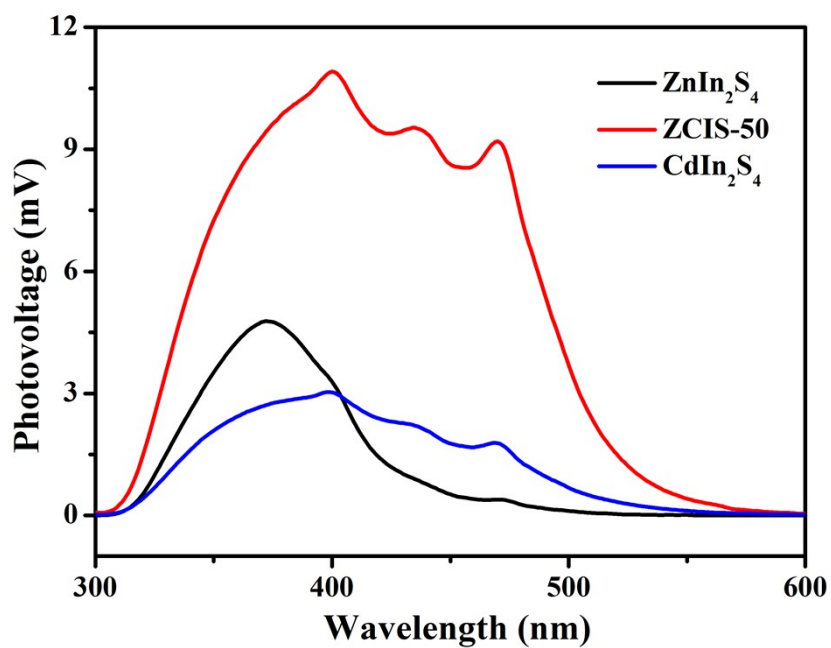


**Figure S7.** Steady-state SPV spectra of ZnIn<sub>2</sub>S<sub>4</sub>, ZCIS-50 and CdIn<sub>2</sub>S<sub>4</sub>.

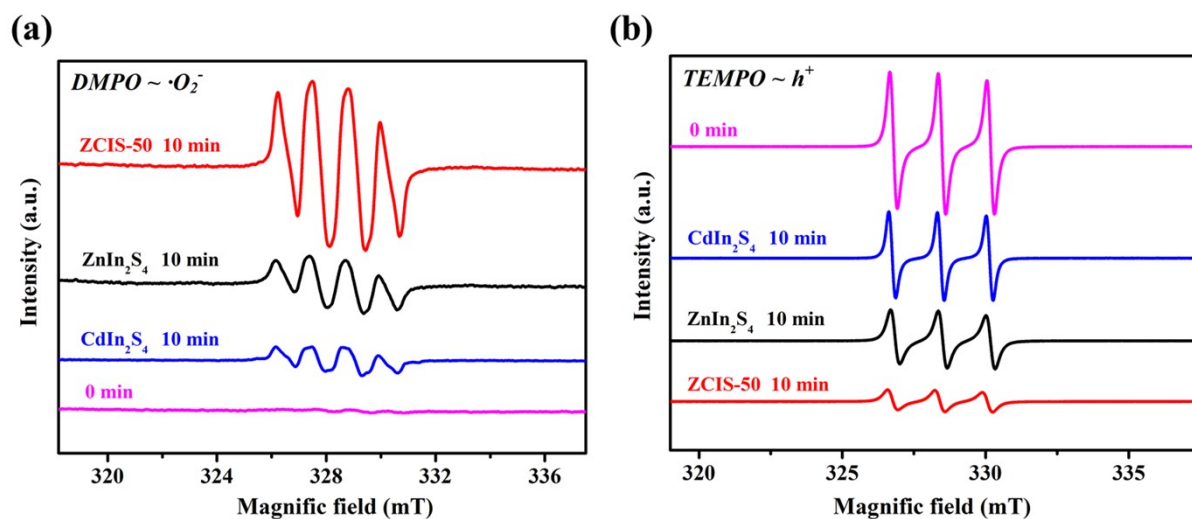


**Figure S8.** EPR spectra of a) DMPO  $\cdot O_2^-$  and b) TEMPO  $h^+$  for ZnIn<sub>2</sub>S<sub>4</sub>, ZCIS-50 and CdIn<sub>2</sub>S<sub>4</sub>.

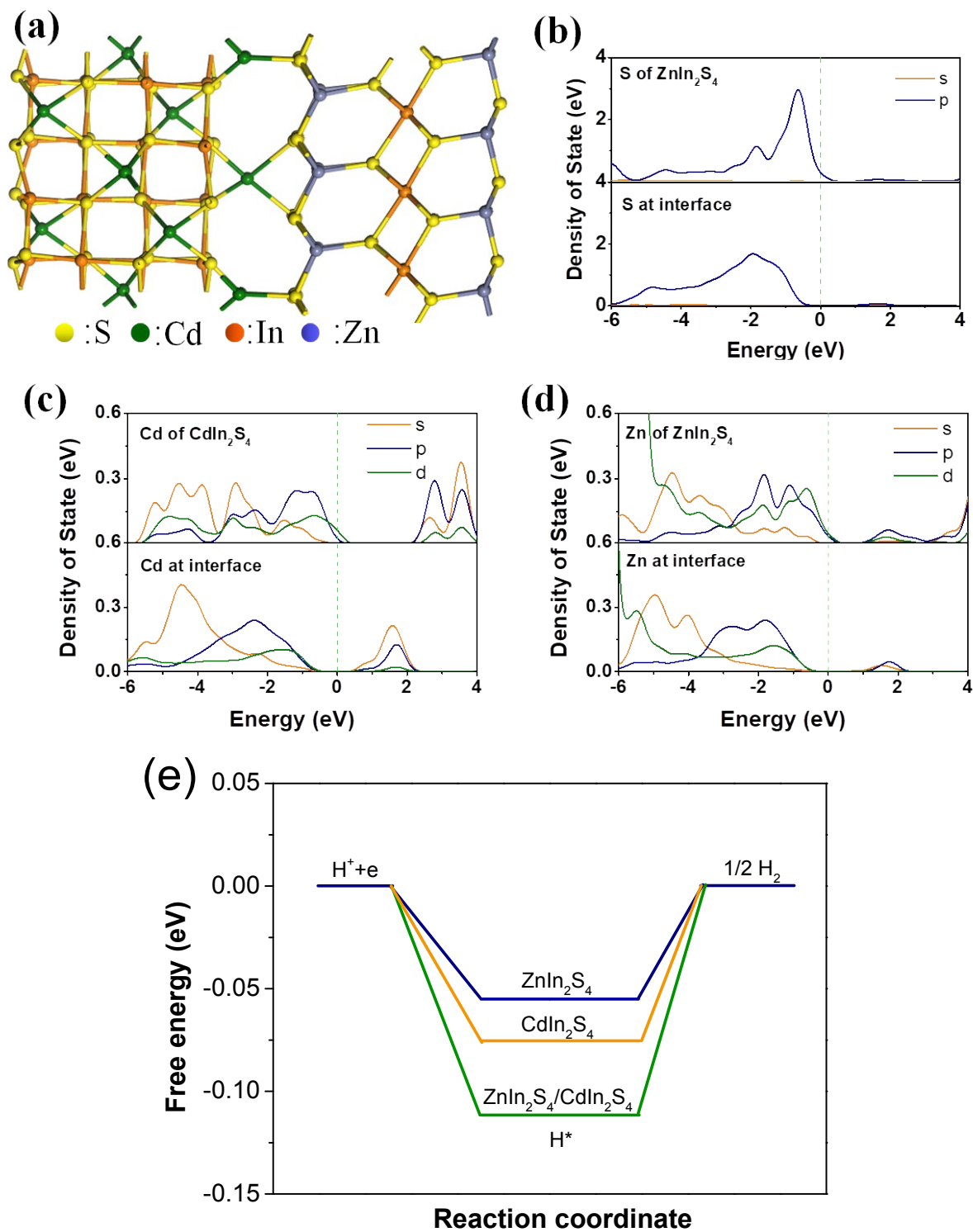
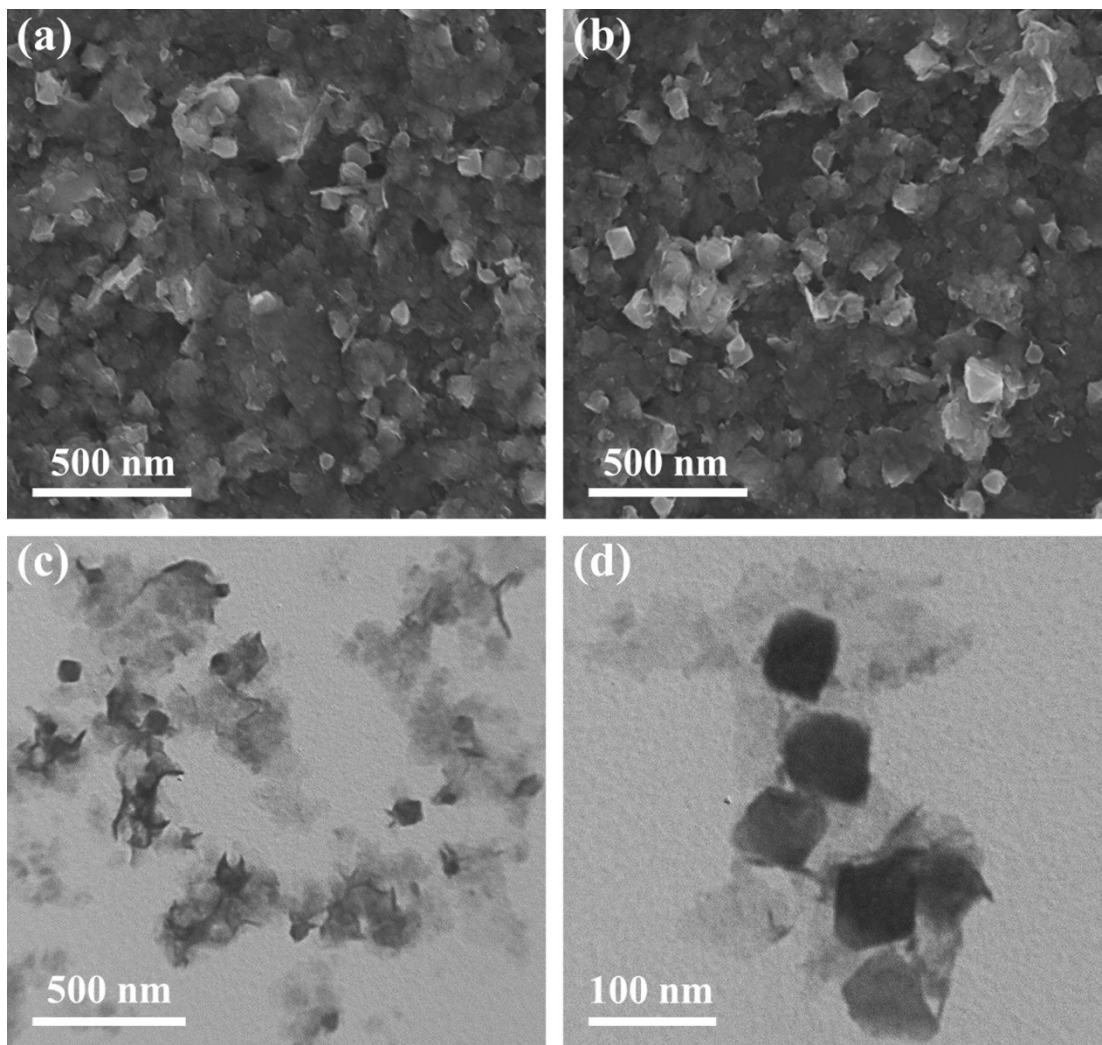
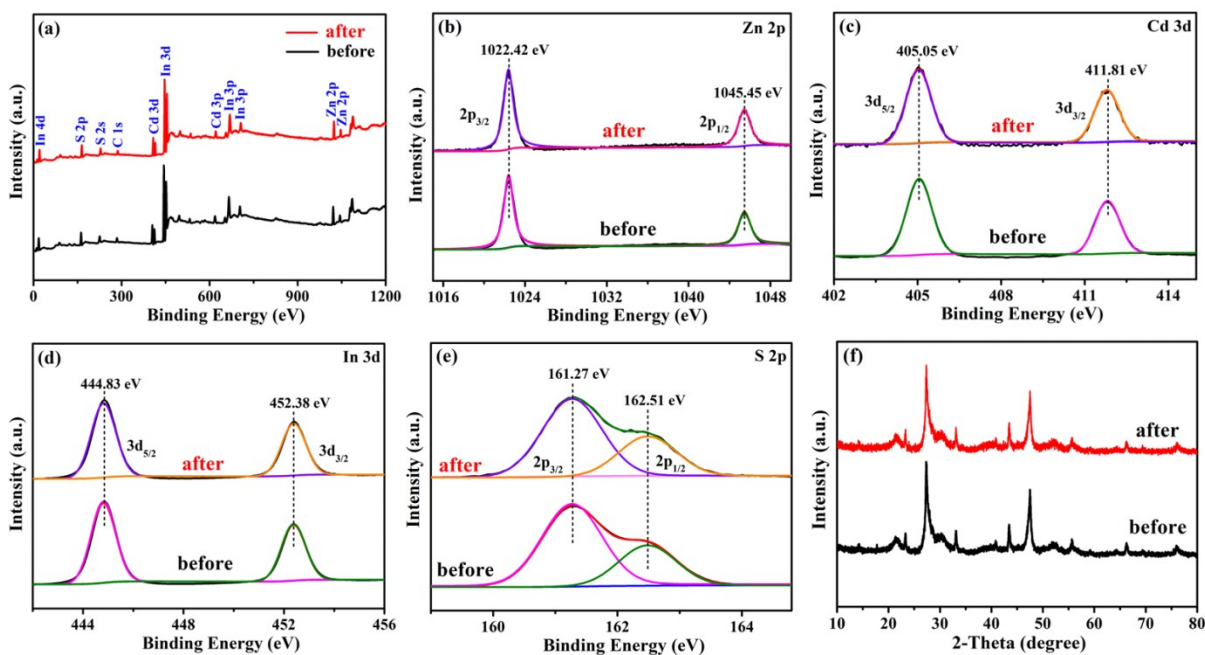


Figure S9 a) The structure model of ZnIn<sub>2</sub>S<sub>4</sub>/CdIn<sub>2</sub>S<sub>4</sub> heterojunction, b) calculated partial density of state of S atom, c) calculated partial density of state of Cd atom, d) calculated partial density of state of Zn atom, e) H\* free energy on ZnIn<sub>2</sub>S<sub>4</sub> (001) and ZnIn<sub>2</sub>S<sub>4</sub>/CdIn<sub>2</sub>S<sub>4</sub> composite.



**Figure S10.** (a,b) SEM and (c,d) TEM images of ZCIS-50 after the cycling photocatalytic reaction in  $\text{Na}_2\text{S}/\text{Na}_2\text{SO}_3$  solution.



**Figure S11.** XPS survey spectrum of ZCIS-50 a) and high-resolution XPS spectra of b) Zn 2p, c) Cd 3d, d) In 3d and e) S 2p for ZCIS-50 before and after recyclability test. f) XRD patterns of before and after recyclability test of ZCIS-50 sample.

**Table S1.** Surface area ( $S_{\text{BET}}$ ), pore volume ( $V_p$ ) and pore diameter ( $D_p$ ) of  $\text{ZnIn}_2\text{S}_4$ , ZCIS-50 and  $\text{CdIn}_2\text{S}_4$  samples.

Sample	$S_{\text{BET}}$ ( $\text{m}^2\cdot\text{g}^{-1}$ )	$V_p$ ( $\text{cm}^3\cdot\text{g}^{-1}$ )	$D_p$ (nm)
$\text{ZnIn}_2\text{S}_4$	83.69	0.233	3.85
ZCIS-50	98.89	0.250	3.79
$\text{CdIn}_2\text{S}_4$	74.37	0.198	3.92

**Table S2.** The nominal and actual atomic ratio in  $\text{ZnIn}_2\text{S}_4$ ,  $\text{CdIn}_2\text{S}_4$  and ZCIS-50 samples.

Sample	Precursor composition (atom ratio of Cd/Zn/In/S)	Composition measured by ICP (atom ratio of Cd/Zn/In/S)
$\text{ZnIn}_2\text{S}_4$	0 : 1 : 2 : 4	0 : 1 : 2.17 : 3.52
ZCIS-50	1 : 1 : 4 : 8	1 : 1.15 : 4.36 : 7.13
$\text{CdIn}_2\text{S}_4$	1 : 0 : 2 : 4	1 : 0 : 2.14 : 3.68

**Table S3.** Time-resolved fluorescence decay parameters of  $\text{ZnIn}_2\text{S}_4$ ,  $\text{CdIn}_2\text{S}_4$  and ZCIS-50 samples.

Samples	$\tau_1$ (ns)	$A_1$ (%)	$\tau_2$ (ns)	$A_2$ (%)	$\tau_A$ (ns)
$\text{ZnIn}_2\text{S}_4$	2.45	46.73	7.94	53.27	5.37
ZCIS-50	0.53	58.84	4.02	41.16	1.97
$\text{CdIn}_2\text{S}_4$	5.80	69.08	22.49	30.92	10.96

**Table S4.** Comparison of ZCIS-50 with representative reported photocatalysts containing ZnIn<sub>2</sub>S<sub>4</sub> or CdIn<sub>2</sub>S<sub>4</sub> component recently.

Photocatalysts	Light source	Hole Scavenger	H <sub>2</sub> evolution rate (mmol h <sup>-1</sup> g <sup>-1</sup> )
ZnIn <sub>2</sub> S <sub>4</sub> @CuInS <sub>2</sub> <sup>1</sup>	300 W Xe lamp, λ>420 nm	0.35 M Na <sub>2</sub> SO <sub>3</sub> and 0.25 M Na <sub>2</sub> S	0.292
1% CQDs@CdIn <sub>2</sub> S <sub>4</sub> /CdS <sup>2</sup>	UV-vis	TEOA	0.397
ZnIn <sub>2</sub> S <sub>4</sub> -300 <sup>3</sup>	300 W Xe lamp, λ>420 nm	20 vol% TEOA	1.940
In <sub>2</sub> S <sub>3</sub> /CdIn <sub>2</sub> S <sub>4</sub> /In <sub>2</sub> O <sub>3</sub> <sup>4</sup>	225 W Xe lamp, λ>320 nm	0.25 M Na <sub>2</sub> SO <sub>3</sub> and 0.35 M Na <sub>2</sub> S	2.004
Oxygen-Doped ZnIn <sub>2</sub> S <sub>4</sub> <sup>5</sup>	300 W Xe lamp, λ>420 nm	0.25 M Na <sub>2</sub> SO <sub>3</sub> and 0.35 M Na <sub>2</sub> S	2.120
WO <sub>3</sub> /ZnIn <sub>2</sub> S <sub>4</sub> <sup>6</sup>	300 W Xe lamp, λ>420 nm	0.25 M Na <sub>2</sub> SO <sub>3</sub> and 0.35 M Na <sub>2</sub> S	2.202
ZnIn <sub>2</sub> S <sub>4</sub> /Ni <sub>12</sub> P <sub>5</sub> <sup>7</sup>	300 W Xe lamp, λ>420 nm	0.25 M Na <sub>2</sub> SO <sub>3</sub> and 0.35 M Na <sub>2</sub> S	2.263
NH <sub>2</sub> -MIL-125(Ti)@ZnIn <sub>2</sub> S <sub>4</sub> /CdS <sup>8</sup>	300 W Xe lamp, λ>400 nm	20 vol% MeOH	2.367
30UiO-66/CdIn <sub>2</sub> S <sub>4</sub> <sup>9</sup>	150 W Xe lamp, λ>420 nm	10 vol% MeOH	2.950
5% CuInS <sub>2</sub> /ZnIn <sub>2</sub> S <sub>4</sub> <sup>10</sup>	300 W Xe lamp, λ>420 nm	0.25 M Na <sub>2</sub> SO <sub>3</sub> and 0.35 M Na <sub>2</sub> S	3.430
Cubic quantum dot/hexagonal microsphere ZnIn <sub>2</sub> S <sub>4</sub> <sup>11</sup>	300 W Xe lamp, λ>420 nm	0.25 M Na <sub>2</sub> SO <sub>3</sub> and 0.35 M Na <sub>2</sub> S	3.806
ZnIn <sub>2</sub> S <sub>4</sub> /NH <sub>2</sub> -UiO-66/5%-MoS <sub>2</sub> <sup>12</sup>	300 W Xe lamp, λ>400 nm	10 vol% TEOA	5.69
Co <sub>9</sub> S <sub>8</sub> @ZnIn <sub>2</sub> S <sub>4</sub> <sup>13</sup>	300 W Xe lamp, λ>400 nm	16.7 vol% TEOA	6.25
ZnS/CdIn <sub>2</sub> S <sub>4</sub> /rGO <sup>14</sup>	300 W Xe lamp, λ>420 nm	16.7 vol% TEOA	6.82
MoS <sub>2</sub> QDs@Vs-M-ZnIn <sub>2</sub> S <sub>4</sub> <sup>15</sup>	300 W Xe lamp, λ>320 nm	10 vol% Lactic acid	6.884
ZnIn <sub>2</sub> S <sub>4</sub> /In(OH) <sub>3</sub> -NiS <sup>16</sup>	300 W Xe lamp, λ>420 nm	4 vol% Lactic acid	7.01
TiO <sub>2</sub> /CdIn <sub>2</sub> S <sub>4</sub> <sup>17</sup>	300 W Xe lamp, λ>420 nm	0.25 M Na <sub>2</sub> S and 0.35 M Na <sub>2</sub> SO <sub>3</sub>	7.86
NiS/Vs-ZnIn <sub>2</sub> S <sub>4</sub> /WO <sub>3</sub> <sup>18</sup>	300 W Xe lamp, λ>400 nm	10 vol% Lactic acid	11.09
Co/NGC@ZnIn <sub>2</sub> S <sub>4</sub> <sup>19</sup>	300 W Xe lamp, λ>400 nm	16.7 vol% TEOA	11.27
ZnIn <sub>2</sub> S <sub>4</sub> /CdIn <sub>2</sub> S <sub>4</sub> (20%)-CC <sup>20</sup>	500 W Xe lamp, λ>420 nm	0.70 M Na <sub>2</sub> S and 0.50 M Na <sub>2</sub> SO <sub>3</sub>	11.29
<b>ZCIS-50 (This work)</b>	<b>300 W Xe lamp, λ&gt;420 nm</b>	<b>0.25 M Na<sub>2</sub>SO<sub>3</sub> and 0.35 M Na<sub>2</sub>S</b>	<b>12.67</b>

## Notes and references

1. X. Guo, Y. Peng, G. Liu, G. Xie, Y. Guo, Y. Zhang and J. Yu, *The Journal of Physical Chemistry C*, 2020, **124**, 5934-5943.
2. J. Huang, L. Li, J. Chen, F. Ma and Y. Yu, *International Journal of Hydrogen Energy*, 2020, **45**, 1822-1836.
3. X. Shi, L. Mao, P. Yang, H. Zheng, M. Fujitsuka, J. Zhang and T. Majima, *Applied Catalysis B: Environmental*, 2020, **265**, 118616.
4. D. Ma, J. W. Shi, Y. Zou, Z. Fan, J. Shi, L. Cheng, D. Sun, Z. Wang and C. Niu, *Nanoscale*, 2018, **10**, 7860-7870.
5. W. Yang, L. Zhang, J. Xie, X. Zhang, Q. Liu, T. Yao, S. Wei, Q. Zhang and Y. Xie, *Angewandte Chemie International Edition*, 2016, **55**, 6716-6720.
6. P. Tan, A. Zhu, L. Qiao, W. Zeng, Y. Ma, H. Dong, J. Xie and J. Pan, *Inorganic Chemistry Frontiers*, 2019, **6**, 929-939.
7. D. Zeng, Z. Lu, X. Gao, B. Wu and W.-J. Ong, *Catalysis Science & Technology*, 2019, **9**, 4010-4016.
8. S. Zhang, M. Du, Z. Xing, Z. Li, K. Pan and W. Zhou, *Applied Catalysis B: Environmental*, 2020, **262**, 118202.
9. R. Bariki, D. Majhi, K. Das, A. Behera and B. G. Mishra, *Applied Catalysis B: Environmental*, 2020, **270**, 118882.
10. Z. Guan, J. Pan, Q. Li, G. Li and J. Yang, *ACS Sustainable Chemistry & Engineering*, 2019, **7**, 7736-7742.
11. J. Wang, Y. Chen, W. Zhou, G. Tian, Y. Xiao, H. Fu and H. Fu, *Journal of Materials Chemistry A*, 2017, **5**, 8451-8460.
12. Q. Ran, Z. Yu, R. Jiang, L. Qian, Y. Hou, F. Yang, F. Li, M. Li, Q. Sun and H. Zhang, *Catalysis Science & Technology*, 2020, **10**, 2531-2539.
13. S. Wang, B. Y. Guan, X. Wang and X. W. D. Lou, *Journal of the American Chemical Society*, 2018, **140**, 15145-15148.
14. C. Xue, H. An, X. Yan, J. Li, B. Yang, J. Wei and G. Yang, *Nano Energy*, 2017, **39**, 513-523.
15. S. Zhang, X. Liu, C. Liu, S. Luo, L. Wang, T. Cai, Y. Zeng, J. Yuan, W. Dong, Y. Pei and Y. Liu, *ACS nano*, 2017, **12**, 751-758.
16. L. Ye, Z. Wen, Z. Li and H. Huang, *Solar RRL*, 2020, **4**, 2000027.

17. M. A. Mahadadalkar, S. W. Gosavi and B. B. Kale, *Journal of Materials Chemistry A*, 2018, **6**, 16064-16073.
18. Z. Li, J. Hou, B. Zhang, S. Cao, Y. Wu, Z. Gao, X. Nie and L. Sun, *Nano Energy*, 2019, **59**, 537-544.
19. S. Wang, Y. Wang, S. L. Zhang, S. Q. Zang and X. W. D. Lou, *Advanced materials*, 2019, **31**, e1903404.
20. L. Li, S. Peng, N. Wang, M. Srinivasan, S. G. Mhaisalkar, Q. Yan and S. Ramakrishna, *Small*, 2015, **11**, 2429-2436.